

# Studying the Physicochemical Properties of Water Activated by Microwave-Induced Plasma Jet for Biological and Medical Applications

F.A. NAEIM\* AND H.R. HUMUD

*Department of Physics, College of Science, University of Baghdad, Al-Jadriyah, 10070, Baghdad, Iraq*

Received: 19.04.2023 & Accepted: 16.05.2023

Doi: [10.12693/APhysPolA.144.81](https://doi.org/10.12693/APhysPolA.144.81)

\*e-mail: [farahammar900@gmail.com](mailto:farahammar900@gmail.com)

This work aims to investigate the chemical and physical properties of water activated by a microwave-induced plasma jet in the system. In this work, the activation of water was studied by plasma microwave using argon gas. To study the physical and chemical properties of water, 10 cm<sup>3</sup> of distilled water was placed in a container made of glass in the form of a dish with a diameter of 5 cm and a depth of 1 cm. The system operates by microwave, with a sustain voltage to the magnetron of 150 V and exposure times ranging from 1 to 10 min. Underflows of 0.7, 1.0, 1.5, and 2.1 l/min of reactive oxygen/nitrogen species types were measured using kits purchased from an American manufacturer, Bartovation, for this purpose. The results showed the concentrations of NO<sub>2</sub>, NO<sub>3</sub>, and H<sub>2</sub>O<sub>2</sub>, increasing with time as well as with the flow rate. With the exposure time, the pH decreases until it reaches 4, and the temperature increases until it reaches 37.2°C; however, the pH increases with the storage time, and the water reaches its natural state with a pH of 7 after 24 h of storage. The concentration of NO<sub>2</sub> and NO<sub>3</sub> increases slightly, and after 6 h, it begins to decrease exponentially, reaching a value close to zero after the passage of 24 h. From that, it can be concluded that the microwave-induced plasma jet system can produce reactive oxygen/nitrogen species, which can be used for biological applications.

topics: plasma activated water (PAW), plasma jet system, microwave discharges, microwave plasma

## 1. Introduction

Plasma is a quasi-neutral gas of charged and neutral particles that exhibit collective behavior. When defining plasma as the fourth state of matter, it is important to recognize the other states of matter. There are three states of matter: solid, liquid, and gas [1]. The temperature of neutral and positively charged species in non-thermal plasma is low; however, the temperature of electrons is substantially higher since electrons are light and rapidly accelerated by applied electromagnetic fields [2]. Many researchers are interested in non-thermal atmospheric pressure plasmas because they have many advantages over low-pressure plasmas [3]. Plasma-activated water (PAW) is one of the most important methods in biological applications. So cold atmospheric-pressure plasma at or near room temperature creates many reactive oxygen species (ROS) and reactive nitrogen species (RNS), such as hydrogen peroxide (H<sub>2</sub>O<sub>2</sub>), singlet oxygen (O<sub>2</sub>), ozone (O<sub>3</sub>), nitric oxide (NO), and hydroxyl radical (OH), as well as electrons, ions, and photons. These things make plasma a good choice for medical and environmental purposes [4]. Plasma-

activated water, prepared by non-thermal plasma treatment of distilled water, has gained increasing attention as an aqueous disinfectant. Various plasma sources are used to activate the water, including direct current (DC), low-frequency discharge, radio frequency discharge, pulsed coronas, dielectric barrier discharge, atmospheric pressure plasma jets, and microwave discharge [5, 6]. Microwave discharges produce non-equilibrium plasma since the electrons can respond to the oscillations of the electric field, whereas the ions are not able to respond due to their large mass. So most of the microwave energy goes preferentially to the electrons, which then produce plasma far from thermodynamic equilibrium [7]. Non-thermal plasma can be used directly in disinfection and sterilization applications, dermatology, cancer treatment, dentistry, anti-bacterial and anti-fungal treatment, and wound healing [5, 8–10]. Microwave plasma has many applications in various fields, including textiles, gas remediation [11], medicine, and surface modification of polymer and metal surfaces [12]. Atmospheric microwave-induced plasma (MIP) has been investigated for decades because of its numerous advantages, such as the absence

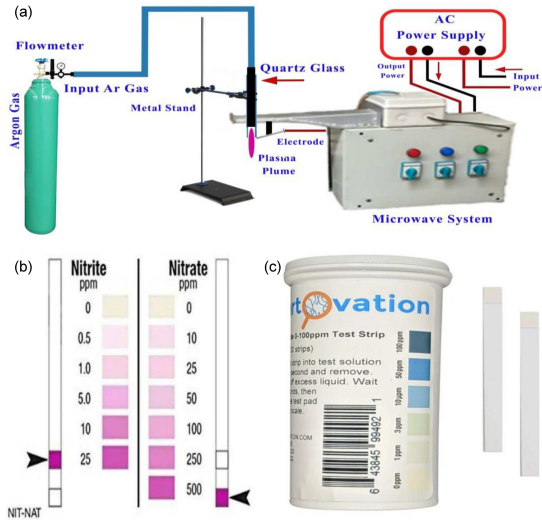


Fig. 1. (a) The schematic diagram of the atmospheric MIPJ system. (b) The strips used (nitrite 0–25 ppm, nitrate 0–500 ppm). (c) Hydrogen peroxide  $H_2O_2$  test strips, low level, 0–100 ppm).

of the need for pricey vacuum equipment, inexpensive, straightforward systems, and simplicity of use [13, 14]. Gao et al. [15] studied the fundamentals of plasma generation, physicochemical properties, and characterization of PAW. They studied the optimization of cold plasma activation by microbubbles. They then critically reviewed processing conditions by PAW, the effectiveness of PAW for biofilm removal, food processing, plant growth in agriculture, and the environment [16]. Samuel Hereinto et al. [16] studied PAW applications for enhanced food safety (both biological and chemical safety). The subsequent effects on food quality (chemical, physical, and sensory properties) are discussed in detail [15].

## 2. Experimental work

A microwave-induced plasma jet (MIPJ) system with a simple design was created utilizing low-cost equipment found in local markets. The 2.45 GHz microwave generator (magnetron type, Panasonic 2M210) was connected to a tapered rectangular waveguide manufactured in the lap. The atmospheric MIPJ system we created in our lab is depicted in Fig. 1a. The tapered rectangular waveguide was tapered from one side to 72 mm (5 mm) to boost the electric field strength in the region of interest to nearly 2.6 times its original value. The discharge tube is a quartz tube with an inner diameter of 6 mm, placed perpendicularly to the waveguide’s wide wall, as shown in Fig. 1a. We exposed  $10\text{ cm}^3$  of sterilized water to microwave plasma; the exposure time ranged from 1 to 10 min, the argon gas flow rate was 0.7, 1.0, 1.5, and 2.1 l/min, and the sustain voltage to the magnetron was 150 V.

TABLE I

Total concentrations of  $NO_2$ ,  $NO_3$ , and  $H_2O_2$  for different gas flow rate values.

Time [min]	$NO_2$	$NO_3$	$H_2O_2$	Total concentrations
Gas flow rate of 0.7 l/min				
0	0	0	0	0
2	5	50	1	56
4	5	100	3	108
6	10	100	3	113
8	10	100	10	120
10	10	100	10	120
Gas flow rate of 1.0 l/min				
0	0	0	0	0
2	5	50	0	55
4	10	100	1	111
6	25	100	3	138
8	25	250	1	276
10	25	250	1	276
Gas flow rate of 1.5 l/min				
0	0	0	0	0
2	0.5	50	10	60.5
4	1	100	10	111
6	1	50	50	101
8	5	50	100	155
10	5	50	100	155
Gas flow rate of 2.1 l/min				
1	0	0	0	0
2	0.5	10	10	20.5
4	0.5	25	10	35.5
6	1	50	100	151
8	1	100	100	201
10	1	100	100	201

To measure the concentration of nitrite ( $NO_2$ ) and nitrate ( $NO_3$ ), the test strip must be dipped into the solution for 2–3 s, removed, shaken to remove excess liquid, and after 30 s compared to the color chart. As shown in Fig. 1b, the  $H_2O_2$  kits can be used by dipping a test strip into the solution for 1 s and removing it. The test pad should be shaken to remove the excess liquid and after 10 s compared to the color scale, as shown in Fig. 1c. After that, the concentrations of  $NO_2$ ,  $NO_3$ , and  $H_2O_2$  were measured as a function of exposure time and flow rate of argon gas, using special kits for this purpose. A pH and temperature measurement was also conducted on the water. The acidity was measured with a pH scale, and the temperature was measured using an infrared (IR) thermometer. The concentrations of  $NO_2$ ,  $NO_3$ ,  $H_2O_2$ , and acidity were also measured after stopping exposure to plasma and for different

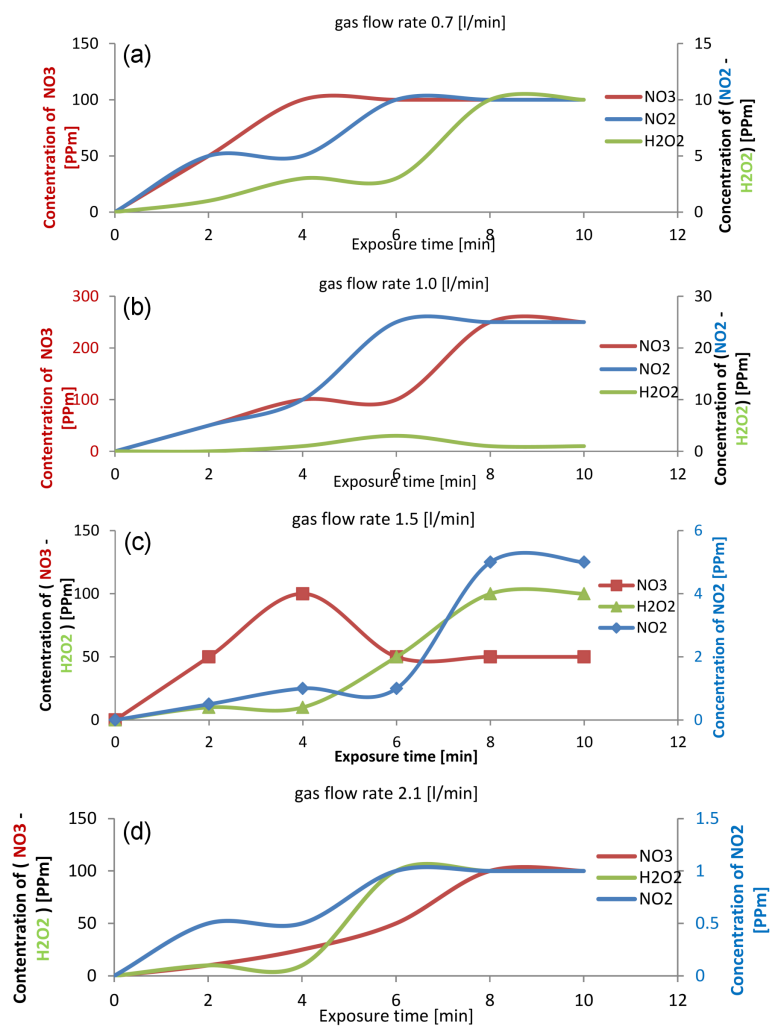


Fig. 2. The relationship between the concentration of NO<sub>2</sub>, NO<sub>3</sub>, H<sub>2</sub>O<sub>2</sub> in units [ppm] and the exposure time at argon gas flow rate (a) for gas flow rate of 0.7 l/min, (b) gas flow rate of 1.0 l/min, (c) gas flow rate of 1.5 l/min, and (d) gas flow rate of 2.1 l/min.

periods to determine the effect of storage on the chemical and physical properties of the activated water.

### 3. Results and discussion

Figure 2 shows the relationship between the concentrations of NO<sub>2</sub>, NO<sub>3</sub>, and H<sub>2</sub>O<sub>2</sub> in units of ppm and the exposure time at argon gas flow rates of (a) 0.7 l/min, (b) 1.0 l/min, (c) 1.5 l/min, and (d) 2.1 l/min. In Fig. 2a, one can notice that each of the concentrations of NO<sub>2</sub>, NO<sub>3</sub>, and H<sub>2</sub>O<sub>2</sub> increases with increasing exposure time and reaches its highest value at slightly different times. This difference is due to the difference in the half-life of these active species, and in addition to that, there is the conversion between these active species. In Fig. 2b–d, we notice that the concentrations of the active species, NO<sub>2</sub>, NO<sub>3</sub>, and H<sub>2</sub>O<sub>2</sub>, increase and decrease dramatically with the exposure time. Table I shows the

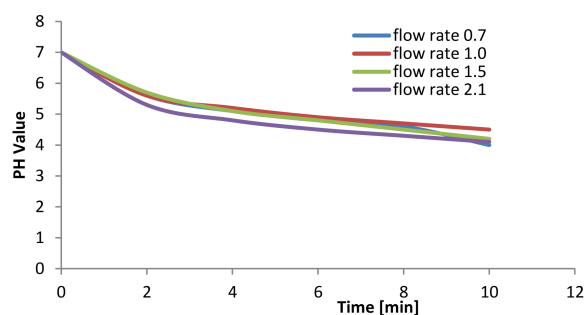


Fig. 3. The relationship between the pH and the exposure time at argon gas flow rate 0.7, 1.0, 1.5 and 2.1 l/min.

total concentrations of NO<sub>2</sub>, NO<sub>3</sub>, and H<sub>2</sub>O<sub>2</sub> for different gas flow rates. From Fig. 2a–d and Table I, it is clear that there are four main factors that controls the concentrations of the active elements NO<sub>2</sub>, NO<sub>3</sub>, and H<sub>2</sub>O<sub>2</sub>. The first factor is the exposure time; the longer the time, the greater the concen-

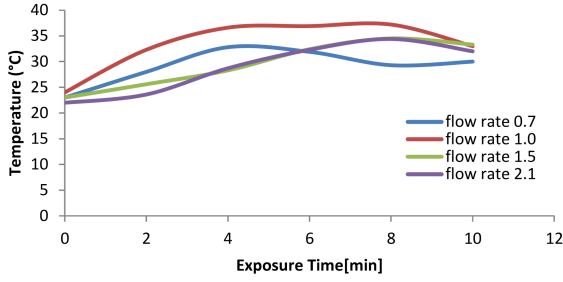


Fig. 4. The relationship between the the water temperature and the exposure time at argon gas flow rate of 0.7, 1.0, 1.5 and 2.1 l/min.

tration of the active species  $\text{NO}_2$ ,  $\text{NO}_3$ ,  $\text{H}_2\text{O}_2$ , and the best irradiation time is 8 min. The second factor is the flow rate. At the best flow rate, i.e., 1.0 l/min, the flow is laminar and does not contain swirls. At flow rates greater than 1 l/min, the gas flow velocity increases, which leads to the displacement of atmospheric air located in front of the plasma jet and, thus, a decrease in the percentage of atmospheric gas. The percentage of Ar gas is higher because the system works with argon gas. The third factor is the difference in the half-lives of  $\text{NO}_2$ ,  $\text{NO}_3$ ,

and  $\text{H}_2\text{O}_2$ , where the longest-lived is  $\text{H}_2\text{O}_2$ , followed by  $\text{NO}_3$ , and the shortest-lived is  $\text{NO}_2$ . The fourth factor is the possibility of converting  $\text{NO}_2$  into  $\text{NO}_3$  through a series of chemical reactions that are sustained by plasma. From Table I, one can notice that the best irradiation time is 8 min, as we get the largest amount of active elements  $\text{NO}_2$ ,  $\text{NO}_3$ , and  $\text{H}_2\text{O}_2$ , at this time. The best flow rate is 1.0 l/min.

Figure 3 shows the relationship between the pH and exposure time. At flow rates of 0.7, 1.0, 1.5, and 2.1 l/min, as shown in the figure, we notice a decrease in the pH from 7 to 4 during 10 min of exposure, and the behavior is similar in all four cases of flow. The low pH was due to the plasma treatment of water, where the treatment leads to the formation of compounds that increase the acidity of the water, such as nitric acid, which in turn results from the interaction of  $\text{NO}_3$  with hydrogen, which results from the dissolution of water by the effect of plasma. Acidic solutions are highly effective in reducing the effectiveness of pathogens.

Figure 4 shows the relationship between water temperature and plasma exposure time at a flow rate of 0.7, 1.0, 1.5, and 2.1 l/min. Clearly, there is an increase in the temperature of the water, and the highest temperature the water reached is

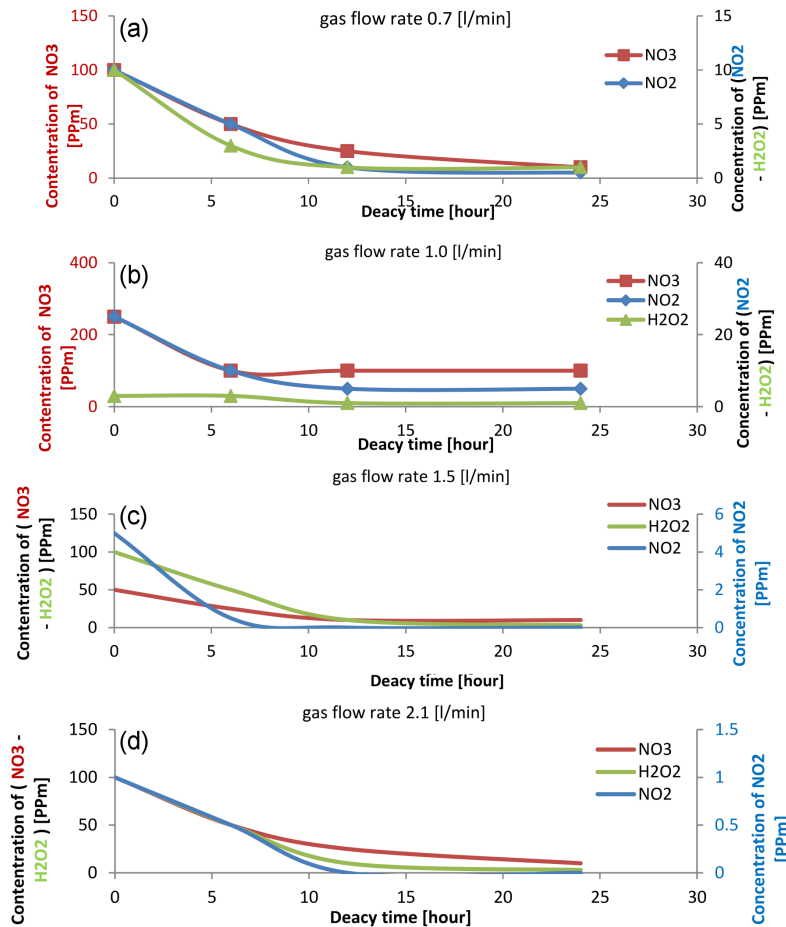


Fig. 5. The relationship between the concentration of  $\text{NO}_2$ ,  $\text{NO}_3$ , and  $\text{H}_2\text{O}_2$  in units [ppm] and the water storage time at different argon gas flow rate; (a) 0.7 l/min, (b) 1.0 l/min, (c) 1.5 l/min, (d) 2.1 l/min.

TABLE II

Total concentrations of  $\text{NO}_2$ ,  $\text{NO}_3$ , and  $\text{H}_2\text{O}_2$  depending on storage time for different values of gas flow rates.

Time [h]	$\text{NO}_2$	$\text{NO}_3$	$\text{H}_2\text{O}_2$	Total concentrations
Gas flow rate of 0.7 l/min				
0	10	100	10	120
6	5	50	3	58
12	1	25	1	27
24	0.5	10	1	11.5
Gas flow rate of 1.0 l/min				
0	25	250	3	278
6	10	100	3	113
12	5	100	1	106
24	5	100	1	106
Gas flow rate of 1.5 l/min				
0	5	50	100	155
6	0.5	25	50	75.5
12	0	10	10	20
24	0	10	3	13
Gas flow rate of 2.1 l/min				
0	1	100	100	201
6	0.5	50	50	100.5
12	0	25	10	35
24	0	10	3	13

about  $37.2^\circ\text{C}$ , which is still not severe and close to room temperature. We also note that the temperature change varies slightly with the flow rate.

In Fig. 5a–d, we notice that the concentrations of  $\text{NO}_2$ ,  $\text{NO}_3$ , and  $\text{H}_2\text{O}_2$  decrease with time and that these reactive species ( $\text{NO}_2$ ,  $\text{NO}_3$ ,  $\text{H}_2\text{O}_2$ ) reach half of their concentration after 6 h of storage at room temperature. As shown in Table II, we also notice that concentrations of all reactive species  $\text{NO}_2$ ,  $\text{NO}_3$ , and  $\text{H}_2\text{O}_2$ , reach small values after 24 h of storage, and this behavior depends on the half-lives of these reactive species ( $\text{NO}_2$ ,  $\text{NO}_3$ ,  $\text{H}_2\text{O}_2$ ).

Figure 6 shows the relationship between the storage time of the PAW and the pH of the activated water at a flow rate of 0.7, 1.0, 1.5, and 2.1 l/min. It is clear from the figure that the pH increases with the storage time, and the water reaches its natural pH of 7 after 24 h of storage. This is because the reactive species have disappeared upon storage and turned into more stable elements and thus the water has returned to its normal state. Figure 7 shows the interaction between water and plasma. A distance of 2 cm separates the plasma torch from the bowl. A glass dish with a diameter of 5 cm and a depth of 1 cm was filled with  $10\text{ cm}^3$  of distilled water.

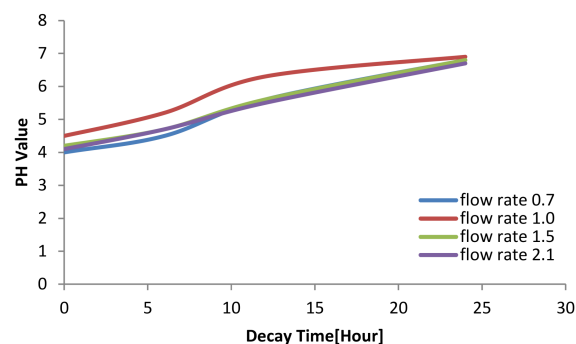


Fig. 6. The relationship between the pH and the water storage time for water activated by plasma at argon gas flow rate of 0.7, 1.0, 1.5, and 2.1 [l/min].



Fig. 7. Water interacting with plasma.

#### 4. Conclusions

From this research, one can conclude the possibility of activating water using a microwave-induced plasma jet. Activation of water leads to the formation of reactive oxygen/nitrogen species (RONS) in water, such as  $\text{NO}_2$ ,  $\text{NO}_3$ , and  $\text{H}_2\text{O}_2$ , and the concentration of these species increases with the increase in exposure time. There are four main factors that control the concentration of the active species. The first factor is the exposure time. The longer the time, the greater the concentration of the active species, and the best irradiation time is 8 min, as we get the largest amount of active elements at this time. The second factor is the flow rate. The best flow rate is 1.0 l/min, where the flow is laminar. The third factor is the difference in the half-lives of  $\text{NO}_2$ ,  $\text{NO}_3$ , and  $\text{H}_2\text{O}_2$ , where the longest-lived is  $\text{H}_2\text{O}_2$ , followed by  $\text{NO}_3$ , and the shortest-lived is  $\text{NO}_2$ . The fourth factor is the possibility of converting  $\text{NO}_2$  into  $\text{NO}_3$  through a series of chemical reactions that are sustained by plasma. Where the greater amount of the active species was obtained, it was 276 ppm, which is the highest quantity for different flow rates. The best storage time is 6 h. The water temperature rises to  $37.2^\circ\text{C}$ , and pH decreases with exposure time. When stored, the pH increases and after 24 h reaches the same value as

before activation. Activation of water using MIPJ is a simple and environmentally friendly method, so it can be used in medical and biological applications.

### References

- [1] F.F. Chen, *Introduction to Plasma Physics and Controlled Fusion*, Vol. 1. Springer, 1984.
- [2] T.P. Kasih, Ph.D. Thesis, Gunma University, 2007.
- [3] T.M.C. Nishime, A.C. Borges, C.Y. Koga-Ito, M. Machida, L.R.O. Hein, K.G. Kostov, *Surf. Coat. Technol.* **312**, 19 (2017).
- [4] L. Guo, R. Xu, L. Gou, Z. Liu, Y. Zhao, D. Liu, L. Zhang, H. Chen, M.G. Kong, *Appl. Environ. Microbiol.* **84**, e00726 (2018).
- [5] M. Moreau, N. Orange, M.G. Feuilleley, *Biotechnol. Adv.* **26**, 610 (2008).
- [6] G.Y. Park, S.J. Park, M.Y. Choi, I.G. Koo, J.H. Byun, J.W. Hong, J.Y. Sim, G.J. Collins, J.K. Lee, *Plasma Sources Sci. Technol.* **21**, 4 (2012).
- [7] B. Eliasson, U.K. Kogelschatz, *IEEE Trans. Plasma Sci.* **19**, 1063 (1991).
- [8] L. Gan, S. Zhang, D. Poorun, D. Liu, X. Lu, M. He, X. Duan, H. Chen, *J. Dtsch. Dermatol. Ges.* **16**, 7 (2018).
- [9] M. Keidar, D. Yan, I.I. Beilis, B. Trink, J.H. Sherman, *Trends Biotechnol.* **36**, 586 (2018).
- [10] C. Hoffmann, C. Berganza, J. Zhang, *Med. Gas Res.* **3**, 1 (2013).
- [11] J. Mizeraczyk, M. Jasiński, H. Nowakowska, M. Dors, *Nukleonika* **57**, 241 (2012).
- [12] Y. Okamoto, *Plasma Sources Sci. Technol.* **5**, 648 (1996).
- [13] H.R. Humud, Q.A. Abbas, A.F. Rauuf, *Int. J. Curr. Eng. Technol* **5**, 2277 (2015).
- [14] C.M. Ferreira, M. Moisan, *Microwave Discharges: Fundamentals and Applications*, Vol. 302, Springer Science & Business Media, 2013.
- [15] Y. Gao, K. Francis, X. Zhang, *Food Res. Int.* **157**, 111246 (2022).
- [16] S. Herianto, C. Hou, C. Lin, H. Chen, *Compr. Rev. Food Sci. Food Saf.* **20**, 583 (2021).